A Low-Power, Programmable Bandpass Filter Section for Higher-Order Filter-Bank Applications

Ravi Chawla*, David W. Graham†, Paul D. Smith‡ and Paul Hasler§
School of Electrical and Computer Engineering
Georgia Institute of Technology, Atlanta, Georgia 30332–0250
Email: *ravic@ece.gatech.edu; †dgraham@ece.gatech.edu; ‡pds@ece.gatech.edu; §phasler@ece.gatech.edu

***Abstract*— We present a programmable continuous-time bandpass filter with center frequencies ranging from 100Hz to 10MHz fabricated in 0.5μm CMOS processes operating at 3.3V supply. This circuit is compact and low power (0.1nW-15μW). SNR was 86dB and 72dB at 1MHz for 2^{nd}- and 4^{th}-order sections with Q's up to 70 (4^{th}-order). We fabricated a 6^{th}- and 10^{th}-order filter-bank chip. We present results for higher-order filters programmed at 1MHz with Butterworth coefficients (passband ripple $<$ 0.5dB).**

I. Motivation for Low-Power, Tunable Filters

With the increasing trend of designing power-efficient analog circuits for portable applications, the demand for analog filters with better performance in terms of speed and power consumption is high. Continuous time filters, particularly $G_m - C$ filters, are the most often used solution for signal frequencies of several MHz [1]. Irrespective of the frequency of operation, $G_m - C$ filters suffer from limited linearity, a large overhead of tuning circuitry and offsets due to device mismatch [2], [3]. In addition, traditional $G_m - C$ filter implementations based on OTAs are area-intensive, thus making them unsuitable for filter-bank applications.

To address these issues, we present a programmable continuous-time bandpass filter topology that is compact and power-efficient. The programmable filter element incorporates our programmable CMOS technology to set accurate time-constants and eliminate offsets [4]. Our programmable analog technology is based upon our modified EEPROM elements designed to work in a standard CMOS technology [5]. The on-chip programming overhead is small as compared to commonly used tuning circuitry that is both power and area intensive [2], [3].

Figure 1 shows the circuit schematic of our core programmable 2^{nd}-order filter element, which was developed from the autozeroing floating-gate amplifier [6]. The common-mode feedback circuit is a standard differential amplifier with high loop-gain [7]. Earlier reports of the filter element demonstrated basic functionality and potential application for a bank of these elements [8], [9]. In this paper, we present the design of programmable filter element to operate over a wide range of frequencies and how this element can be used to design higher-order filters. These higher-order filters can also be tuned to desired transfer functions, such as Butterworth and Chebyshev, after the circuit has been fabricated by programming floating-gates.

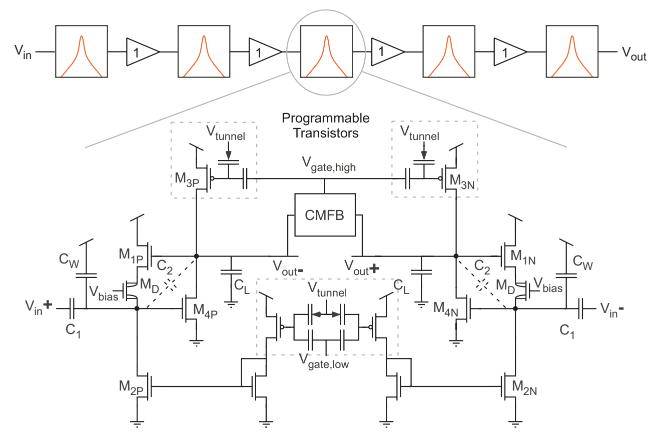

Fig. 1. **Block diagram and schematic of the filter element**: Block diagram of 10^{th}-order filter and circuit schematic of the core filter element. Floating–gate transistors can be programmed to set the desired bias current, thus, accurate time constants and quality factor, Q. All other parameters can also be set using capacitor ratios.

In section II, we discuss the design of the programmable 2^{nd}-order element. We present the measured results for 2^{nd}- and 4^{th}-order filters in section III. Section IV presents the design of a 6^{th}- and 10^{th}-order filter using the core filter section. We also present measured results for the designed filters programmed with Butterworth approximation. We conclude the discussion in section V with a summary of performance.

II. Design Considerations of Programmable Bandpass Element

We now analyze our core programmable filter section and derive the governing design equations. The circuit schematic shown in Fig. 1 can be analyzed using the small-signal model of the differential half-circuit. The transfer function of the filter section is given by

$$\frac{V_{out}}{V_{in}} = -\frac{C_1}{C_2}\frac{\frac{sC_2}{g_{m1}}(1-\frac{sC_2}{g_{m4}})}{s^2\frac{(C_T C_o - C_2^2)}{g_{m1}g_{m4}} + s(\frac{C_2}{g_{m1}} + \frac{C_2}{g_{m4}}(\frac{C_o}{C_2} - 1)) + 1} \quad (1)$$

where the high and low time constants (τ_l and τ_h), and the high-frequency zero (τ_f) can be observed as

$$\tau_l = \frac{C_2}{g_{m1}}, \qquad \tau_h = \frac{(C_T C_o - C_2^2)}{C_2 g_{m4}}, \qquad \tau_f = \frac{C_2}{g_{m4}}$$

The quality factor, Q, and the corner frequency for a particular value of currents are given by:

$$Q = \frac{\sqrt{(C_T C_o - C_2^2) g_{m1} g_{m4}}}{C_2 g_{m4} + C_L g_{m1}}, \qquad \tau = \sqrt{\frac{C_T C_o - C_2^2}{g_{m1} g_{m4}}}$$

The total capacitance, C_T, and the output capacitance, C_O, are defined as $C_T = C_1 + C_2 + C_W$ and $C_O = C_2 + C_L$. Transconductances g_{m1} and g_{m4} depend on the current flowing through transistor M_{1N}, M_{1P}, M_{4P} and M_{4N}. The gain of the filter element is set by capacitor ratios and can, thus, be set accurately. The filter element can be tuned to desired corner frequencies and Q-values by programming the g_{m1} and g_{m4} using the floating–gate current sources [5]. Transistors M_{1N}, M_{1P}, M_{4P} and M_{4N} can operate in sub-threshold or in moderate inversion depending on the desired frequency response. The high-frequency zero, τ_f, is designed such that it is well outside the passband of the filters.

The maximum Q-value occurs when the drawn capacitance C_2 is small in comparison to C_L and can be derived to be

$$Q_{max} \approx \frac{1}{2}\sqrt{\frac{C_T}{C_2}} \tag{2}$$

In the case of no physical capacitance C_2, this capacitance value depends on C_{gd4} and C_{gs1}. The short-channel device, M_D as shown in Fig. 1, helps to increase linearity at the lower corner frequency by source degeneration. M_D also helps in alleviating the effect of C_{gs1} on the value of Q. The linearity at the higher corner can be set by capacitor, C_W, due to capacitive attenuation at the input.

The output referred noise of the 2^{nd}-order section tuned to a particular response is given by :

$$V_{no}^2 = \left(\frac{1}{s^2\tau_l\tau_h + s(\tau_l + \tau_f(\frac{C_o}{C_2} - 1)) + 1}\right)^2 \left[\left(\frac{sC_2 - g_{m4}}{g_{m1}g_{m4}}\right)^2 (I_1^2 + I_2^2) + \left(\frac{sC_T + g_{m1}}{g_{m1}g_{m4}}\right)^2 (I_3^2 + I_4^2)\right] \tag{3}$$

where I_1, I_2, I_3, I_4 are noise currents (thermal and flicker noise contribution) for transistors $M_{1N}, M_{1P}, M_{2N}, M_{2P}, M_{3N}, M_{3P}, M_{4N}$ and M_{4P}, respectively. As can be seen, the transfer function of the noise depends on the response of the filter and the circuit parameters. This expression can be used to design the filter element for good noise performance.

III. Experimental Results for Bandpass Filter Sections

Figure 2 shows the measured frequency response of a 2^{nd}- and 4^{th}-order filter when programmed over decades of frequency. The 4^{th}-order filter was built by cascading two programmable 2^{nd}-order sections. The filter responses can be programmed anywhere from 100Hz to 10MHz. Simulations of the filter sections matched well with the measured response, as can be seen from Fig 2. The measurements were limited to 1MHz due the output buffers (10MHz). Figure 3 shows the filter response of a 2^{nd}-order section when fine-tuned over a small range of frequencies. Figures 2 and 3 show that the filter topology can be both programmed over a wide frequency range and fine tuned over a small frequency range, if required. The designed 2^{nd}- and 4^{th}-order filter sections can be programmed to give Q-values up to 9 and 70, respectively. Figure 4 shows the measured plot of a 4^{th}-order filter tuned at 1MHz to have a Q of 70.

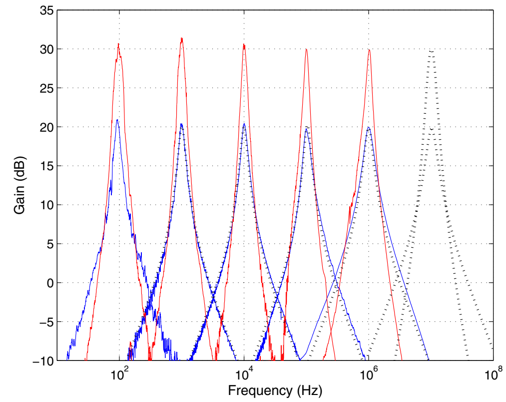

Fig. 2. **Measurement showing the programmed corner frequencies**: The measured frequency response showing that the filter can be programmed over a wide range of frequencies from 10Hz - 10MHz. Results are shown for 2^{nd}- and 4^{th}-order filters. Simulations of the filter, shown as dashed lines, matched well with the measured results.

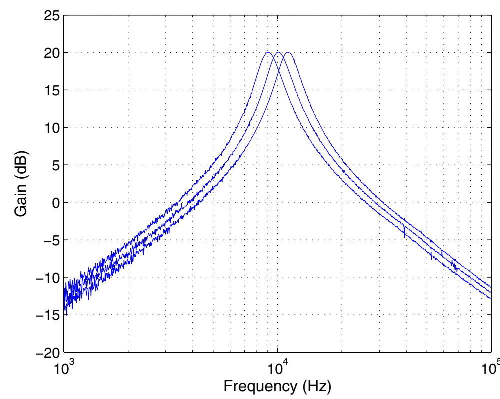

Fig. 3. **Measurement showing tuning of the filter element**: Measured frequency response of 2^{nd}-order filter tuned at 9KHz, 10KHz and 11KHz. Plot shows that the center frequencies can be fine-tuned by setting the desired bias current accurately using floating–gate transistors.

Figure 5 shows the measurement to compute 1-dB compression point for 2^{nd}- and 4^{th}-order sections for two different values of programmed Q's. As expected, the linearity degrades as the Q-value increases. The values of linearity for the 2^{nd}- and 4^{th}-order sections tuned to have a Q of 2.5 and 5.2, respectively, at 1MHz were found to be -24dBm (83mV$_{pp}$) and -42dBm (11.5mV$_{pp}$), respectively. Figure 6 shows the measurement to compute 1-dB compression point for different values of V_{bias} for 2^{nd}-order section programmed to have a low Q. It can be clearly seen that the linearity increases from -8.5dBm to -5dBm as V_{bias} is decreased from 3.3V to 1.9V. This increase in linearity comes at the cost of lowering of the low frequency corner due to the source degeneration effect.

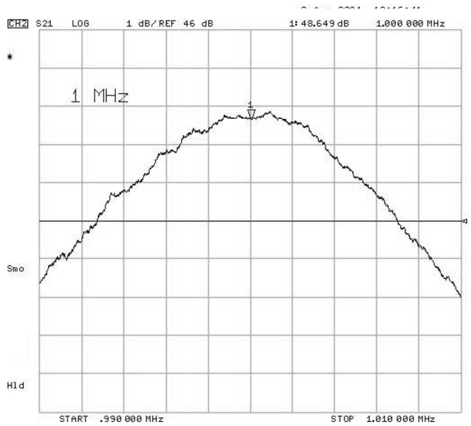

Fig. 4. **Q-tuning measurement**: Measurement showing a Q-value of 70 obtained for a 4^{th}-order filter tuned at 1MHz center frequency. The value of Q can be determined by the 3-dB bandwidth and the center frequency.

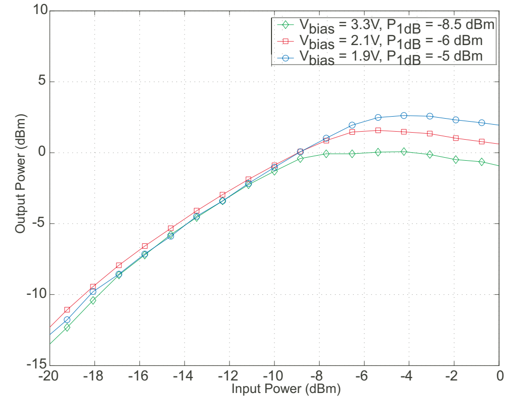

Fig. 6. **Effect of Vbias on linearity**: Measurement showing the improvement in 1-dB compression point as the bias voltage, Vbias, is increased. This increase in linearity is due to the source-degeneration effect.

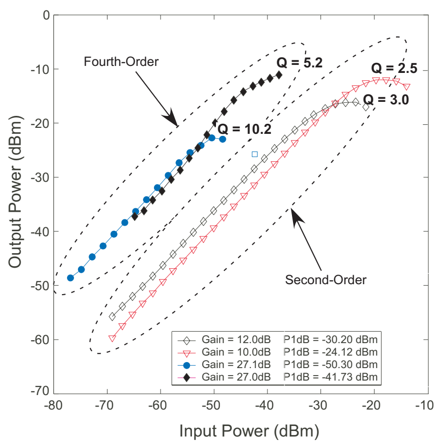

Fig. 5. **1-dB compression measurement**: Measurement to compute 1-dB compression point for different values of Q for 2^{nd}- and 4^{th}-order sections.

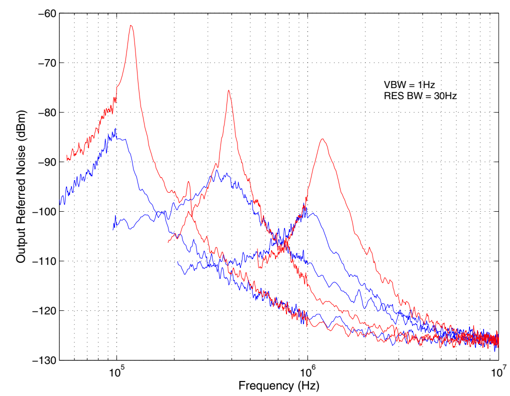

Fig. 7. **Noise measurements for 2^{nd}- and 4^{th}-order sections**: Plot showing the measured output-referred noise spectrums of 2^{nd}- and 4^{th}-order filters tuned at different frequencies.

Thus, the current, I_2, needs to be programmed to a higher value than before to get the same lower time constant.

Figure 7 shows the output-referred noise measurement of the 2^{nd}- and 4^{th}-order filter sections for various programmed corners. The noise spectrum looks like the frequency response of the tuned filter, as expected from (3). Figure 7 also shows that overall noise spectrum decreases as the programmed center frequency is increased. This can be attributed to the 1/f component of the noise spectrum. The measured output spot-noise at 1MHz for 2^{nd}-order section was found to be -100 dBm (using VBW = 1Hz).

IV. High-order Filter Implementation

We used the 2^{nd}-order section, discussed above, in cascade to implement higher-order filters. Figure 1 shows the block diagram of the 10^{th}-order filter using these core 2^{nd}-order sections. These higher order filters can also be tuned to desired transfer functions such as Butterworth and Chebyshev after the circuit has been fabricated. The 2^{nd}-order sections were designed such that the Q_{max} (2) is greater than that required by the higher-order filter specification. The coefficients can be set by accurately programming the floating-gate currents. As is evident from the schematic in Fig. 1, the input capacitance changes with frequency [8]. This becomes a problem when these sections are cascaded. A unity-gain buffer was introduced between each stage, as shown in Fig. 1, to take care of this problem. The buffer was designed to have a good frequency response and linearity and thus, had no effect on the performance of the system. These buffers did add noise to the entire system, however the added noise did not degrade the performance.

Figure 8 shows the frequency response of a 6^{th}- and a 10^{th}-order filter tuned to have a center frequency of 1MHz. These filters can be tuned to have different center frequencies. The limitations in the measurement for high frequency was once again the output driving buffer. The designed 10^{th}-order filter was compact and power efficient. This filter can be used in a variety of filter-bank applications [9], [10]. Figure 9 shows the die photograph of the chip with 16 filters that was used to take the measurements. This chip can be configured as a bank of 6^{th}-order or 10^{th}-order filters depending on the application.

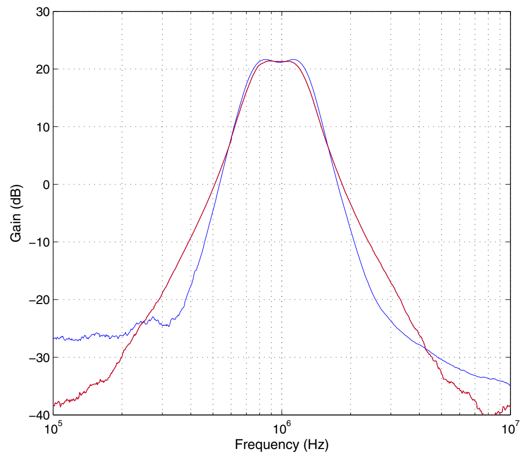

(a)

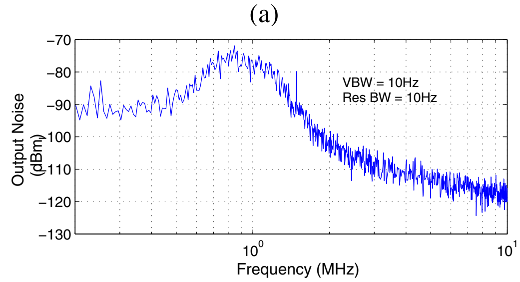

(b)

Fig. 8. **Magnitude response and noise spectrum of a 6^{th}- and 10^{th}-order filter**: (a) Measured magnitude frequency response of a 6^{th}- and 10^{th}-order filter designed using 2^{nd}-order sections. (b) Plot showing output referred noise spectrum for the 10^{th}-order filter.

V. Conclusion

We presented a compact continuous-time ($G_m - C$) bandpass filter circuit that can be programmed to operate from 100Hz to 10MHz center frequencies. Table I summarizes the measured performance of all the filter sections fabricated. We demonstrated the characterization results for the basic 2^{nd}-order and 4^{th}-order sections designed for high Q's. The experimental results presented were from a 0.5μm double-poly CMOS process; these results scale straightforwardly to other CMOS processes. The measurements show an SNR of 86dB and 72dB, respectively, for a 2^{nd}-order and 4^{th}-order section at a center frequency of 1MHz. We obtained Q's as high as 70 from the 4^{th}-order sections. We also presented results for a 6^{th}- and 10^{th}-order filter fabricated by cascading the 2^{nd}-order sections. These filters were programmed at a center frequency of 1MHz to have Butterworth coefficients. The measured SNR was 55dB for the 10^{th}-order filter programmed at 1MHz. The low power consumption and low area make these extremely attractive for filter-bank applications [9], [10].

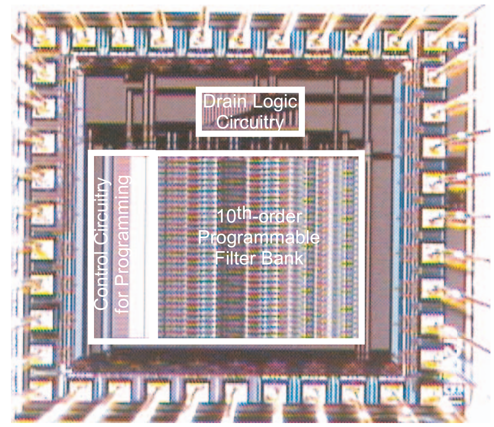

Fig. 9. **Micrograph of the 10^{th}-order filter-bank chip**: Chip micrograph of filter-bank chip, with 16 filters, that was used to measure the 6^{th}- and 10^{th}-order filter response. The chip includes logic and control circuitry that is used for programming. The area of the entire chip was 1.1 mm^2.

TABLE I

Summary of Performance

Parameter	2^{nd}-order	4^{th}-order	10^{th}-order
Frequency Range	100Hz-10MHz	100Hz-10MHz	N/A
Q range	< 9	< 72	N/A
Output Noise (dBm @ 1MHz) (VBW = 1Hz)	-100dBm	-84dBm	-78dBm (VBW = 10Hz)
Total Power (with buffers)	0.1nW-15μW	0.25nW-15μW	20μW @ 1MHz
SNR @ 1MHz	86dB	72dB	55dB
Area	2.1e3μm^2	4.8e3μm^2	13.2e3μm^2
Programming % error	$< \pm 0.2\%$	$< \pm 0.2\%$	$< \pm 0.2\%$
Programming mechanism	Hot–electron injection	and	Fowler-Nordheim tunneling
Tunneling Voltage (V)	15	15	15

References

[1] D. A. Johns and K. Martin, Eds., *Analog Integrated Circuit Design*. New York, NY: John Wiley and Sons, Inc., 1997.

[2] P. Kallam, E. Sanchez-Sinencio, and A. Karsilayan, "An enhanced adaptive q-tuning scheme for a 100-mhz fully symmetric ota-based bandpass filter," *IEEE Journal of Solid-State Circuits*, vol. 38, pp. 585 – 593, April 2003.

[3] T. Pham and P. Allen, "A highly accurate step-response-based successive-approximation frequency tuning scheme for high-q continuous-time bandpass filters," *IEEE Transactions on Circuits and Systems I*, vol. 50, pp. 221 – 227, May 2003.

[4] F. Adil, G. Serrano, and P. Hasler, "Offset removal using Floating-Gate circuits for Mixed-Signal Systems," in *Proceedings of the IEEE Southwest Symposium on Mixed-Signal Design*, Feb 2003.

[5] G. Serrano, P. Smith, H. Lo, R. Chawla, T. Hall, C. Twigg, and P. Hasler, "Automated Rapid Programming of Large Arrays of Floating-gate Elements," in *Proceedings of the International Symposium on Circuits and Systems*, vol. I, May 2004, pp. 373–376.

[6] P. Hasler, B. A. Minch, C. Diorio, and C. A. Mead, "An autozeroing floating-gate amplifier," *IEEE Transactions on Circuits and Systems II: Analog and Digital Signal Processing*, vol. 48, no. 1, 2001.

[7] R. Chawla, G. Serrano, D. Allen, A. Periera, and P. Hasler, "Fully differential floating-gate programmable otas with novel common-mode feedback," in *Proceedings of the International Symposium on Circuits and Systems*, vol. I, May 2004, pp. 817–820.

[8] P. D. Smith, D. W. Graham, R. Chawla, and P. Hasler, "A five-transistor bandpass filter element," in *Proceedings of the International Symposium on Circuits and Systems*, vol. I, May 2004, pp. 861–864.

[9] D. W. Graham, P. D. Smith, R. Ellis, R. Chawla, and P. Hasler, "A programmable bandpass array using floating-gate elements," in *Proceedings of the International Symposium on Circuits and Systems*, vol. I, May 2004, pp. 97–100.

[10] C. Salthouse and R. Sarpeshkar, "A practical micropower programmable bandpass filter for use in bionic ears," *IEEE Journal of Solid-State Circuits*, vol. 38, pp. 63 – 70, January 2003.